ISSN (Print) : 0974-6846
Indian Journal of Science and Technology, Vol 10(25), DOI: 10.17485/ijst/2017/v10i25/112309, July 2017 ISSN (Online) : 0974-5645

A Note on Stimulus Gravitational Wave Detection

Farrin Payandeh

Department of Physics, Payame Noor University (PNU), P.O. BOX, 19395-3697 Tehran, Iran;
payandehfarrin92@gmail.com

Abstract

Objectives: To set up a theoretical background for the detection of gravitational waves in a stimulated system. **Methods:** The methods are based on theoretical notions of gravitational waves on a flat background, and regard them as bumps which make links between two different copies of Minkowskian manifolds. Such a bump, is indeed supposed to impose essential impulses to the massive particles, residing on the space-time manifold, giving them reasonable velocities. In our method, such velocities are detected by means of a normal stimulated detector. **Findings:** We find that, the elementary dumbbell oscillators in the detector, initially unexcited, have a cross section for absorption of unpolarized gravitational radiation proportional to a Sin function, and when excited, radiates with intensity also proportional to Sin function. The patterns of emission and absorption are identical. We also find that, any other dumbbell oscillator gives the same pattern, apart from a possible difference of orientation. Considering a nonrotating oscillator of general shape, we deduce that it undergoes free vibrations in a single no degenerate mode. We also find that this emission pattern, apart from a fourth parameter that determines total intensity, is uniquely fixed by a single parameter. Furthermore, we construct systems for the pattern of intensity for the two extreme values of this parameter and for a natural choice of parameter intermediate between these two extremes. **Applications:** we obtain the parameter in question in terms of a certain dimensionless combination of the principal moments of the reduced quadrupole tensor. The method we introduce here is applicable along with the technical difficulties to be surmounted in constructing gravitational wave detectors.

Keywords: Detection, Gravitational Waves, Quanrupole Tensor, Resonance, Stimulation, Vibration

1. Introduction

An independent approach in modern physics of any symmetry considerations at all is the study of a gravitational wave. Just as identical to water waves of small ripples rolling across the ocean, the name gravitational waves derive for their small ripples rolling across spacetime[1-5]. Space time is similar. Propagating through the universe, according to Einstein's theory, must be a complex pattern of small-scale ripples in the space time curvature. These ripples are produced by binary stars, by supernovae, by gravitational collapse, by explosions in galactic nuclei. Locally, one can ignore the interaction of these ripples with the large-scale curvature of space-time and their nonlinear interaction with each other. One can pretend the waves propagate in flat space-time; and one can write down a simple wave equation for them. But globally one cannot. The large-scale curvature due to quiescent stars and galaxies will produce redshifts and will deform wave fronts; and the energy carried by the waves themselves will help to produce the large-scale curvature. The gravitational waves of our universe as propagating through flat, empty space time (local viewpoint). Then they can be analyzed using the linearized theory of gravity, which has an extant availability in texts on general relativity and its astrophysical consequences[6-10]. Linearized theory, one recalls, is a weak-field approximation to general relativity. The equations of linearized theory are written and solved as though space time were flat (special-relativity viewpoint); but the connection to experiment is made through the curved-space formalism of general relativity.

In the recent years, a huge attempt has been devoted to detect the gravitational waves, which finally led to their detection in 2016[11]. A gravitational wave detector is even easier to analyze than the generator (for example, a binary system or a black-hole) when one deals with gravitational waves within the framework of general relativity. Potential detectors are usually installed in the solar system, where gravity is so weak and space-time so nearly flat that a plane gravitational wave coming in remains for all

** Author for correspondence*

practical purposes a plane gravitational wave. Moreover, the nearest source of significant waves is so far away that, for all practical purposes, one can consider the waves as plane-fronted when they reach the Earth. Consequently, as they propagate in the z -direction past a detector, they can be described to high accuracy by the transverse-traceless linearized expressions. Because of the increasing importance of constructing gravitational waves detectors, we deal with the possible ways of building such detectors, in a mathematical viewpoint. The paper is organized as follows: In Section 2, we consider a resonant detector based on a definite pattern of an ideal detector. In Section 3, we assume that this detector obeys polarized wave equations in the $E_{\text{vibration}} \gg kT$ limit. In Section 4, we take into account small displacements and solve the wave equations which results in the determinations of the massive approximation. We conclude in Section 5.

2. The Idealized Resonant Detector

We consider the proper reference frame of a vibrating-bar detector. In such detectors, the bar hangs by a wire from a cross beam, which is supported by vertical posts (Figure 1) that are embedded in the Earth. Consequently, the bar experiences a 4-acceleration given, by $\mathbf{a} = g(\partial / \partial \hat{z})$, where g is the local acceleration of gravity. Later, the spatial axes will have rotated relative to the bar, so the components of $\mathbf{a}$ but not its magnitude will have changed. The proper reference frame relies on an imaginary clock and three imaginary gyroscopes located at the bar's center of mass. Coordinate time is equal to proper time as measured by the clock, and the directions of the spatial axes $\partial / \partial x^{\hat{j}}$ are attached to the gyroscopes. The forces that prevent the gyroscopes from falling in the Earth's field must be applied at the centers of mass of the individual gyroscopes.

The metric perturbation results in the Riemann tensor perturbations

$$h_{xx}^{TT} = -h_{yy}^{TT} = A_+(t-z), h_{xy}^{TT} = h_{yx}^{TT} = A_\times(t-z), \tag{1}$$

$$R_{x0x0} = -R_{y0y0} = -\frac{1}{2}\ddot{A}_+(t-x), \tag{2}$$

$$R_{x0y0} = R_{y0x0} = -\frac{1}{2}\ddot{A}_\times(t-z).$$

These together, give the following stress-energy tensor:

$$T_{00}^{(\mathrm{GW})} = T_{zz}^{(\mathrm{GW})} = -T_{0z}^{(GW)} = \frac{1}{16\pi}\left\langle \dot{A}_+^2 + \dot{A}_\times^2 \right\rangle_{\text{time average}}. \tag{3}$$

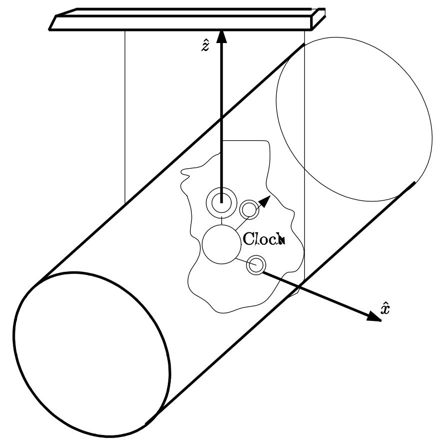

Figure 1. A schematic view of the vibrating bar detector.

To analyze most easily the response of the detector to these impinging waves, use not the TT coordinate system $\{x^\alpha\}$ (which is specially "tuned" to the waves), but rather use coordinates $\{x^{\hat{\alpha}}\}$, specially "tuned" to the experimenter and his detector. The detector might be a vibrating bar, or the vibrating Earth, or a loop of tubing filled with fluid. But whatever it is, it will have a center of mass. Attached the spatial origin, $x^{\hat{j}} = 0$, to this center of mass; and attach orthonormal spatial axes, $\partial / \partial x^{\hat{j}}$, to gyroscopes located at this spatial origin. If the detector is accelerating (i.e., not falling freely on a geodesic curve), make the gyroscopes accelerate with it by applying the necessary forces at their centers of mass. Use, as time coordinate, the proper time $x^{\hat{0}} = \tau$ measured by a clock at the spatial origin. Finally, extend these locally defined coordinates $x^{\hat{\alpha}}$ throughout all space time in the straightest manner possible.

Now let the 4-velocity, i.e. the tangential vector to the trajectory curve, measured by an observer. Whose proper time is measured by the parameter τ, be denoted by u^α. The whole system would therefore obey the evolution equations[12-17]

$$\frac{d\Theta}{d\tau} + \frac{1}{3}\Theta^2 + \sigma^2 - \omega^2 = -R_{\mu\nu}u^\mu u^\nu, \tag{4}$$

$$\frac{d\sigma_{\mu\nu}}{d\tau} = -\frac{2}{3}\Theta\sigma_{\mu\nu} - \sigma_{\mu\lambda}\sigma^\lambda{}_\nu - \omega_{\mu\lambda}\omega^\lambda{}_\nu + \frac{1}{3}h_{\mu\nu}\left(\sigma^2 - \omega^2\right)$$
$$+C_{\lambda\nu\mu\rho}u^\lambda u^\rho + \frac{1}{2}h_{\mu\lambda}h_{\nu\rho}R^{\lambda\rho} - \frac{1}{3}h_{\mu\nu}h_{\lambda\rho}R^{\lambda\rho},$$

$$\frac{d\omega_{\mu\nu}}{d\tau} = -\frac{2}{3}\Theta\omega_{\mu\nu} - 2\sigma^\lambda{}_{[\nu}\omega_{\mu]\lambda},$$

in which, $\Theta, \sigma_{\mu\nu}$ and $\omega_{\mu\nu}$ are respectively the scalar expansion, the symmetric traceless shear tensor and the anti-symmetric rotation tensor. Moreover $\sigma^2 = \sigma_{\mu\nu}\sigma^{\mu\nu}, \omega^2 = \omega_{\mu\nu}\omega^{\mu\nu}$ and $C_{\lambda\nu\mu\rho}$ is the Weyl conformal tensor. Also $h_{\mu\nu}$ is the projection tensor which for time-like curves is defined by

$$h_{\mu\nu} = g_{\mu\nu} + u_\mu u_\nu. \tag{5}$$

The equations (4) deal with the kinematics of flows which are generated by vector fields. Such flows are indeed congruence's of integral curves which may or may not be geodesics. Actually in the context of these equations, we are interested in the evolution of the kinematical characteristics of the so-called flows, not the origin of them. These characteristics which are contained in those equations, may constitute one equation like[18]

$$\nabla_\nu v_\mu = \sigma_{\mu\nu} + \omega_{\mu\nu} + \frac{1}{3}h_{\mu\nu}\Theta, \tag{6}$$

$$\sigma_{\mu\nu} = \nabla_{(\nu}v_{\mu)} - \frac{1}{3}h_{\mu\nu}\Theta,$$

$$\Theta = \nabla_\mu v^\mu,$$

and the antisymmetric part is

$$\omega_{\mu\nu} = \nabla_{[\nu}v_{\mu]}. \tag{7}$$

Geometrically, these quantities are related to a cross-sectional area which encloses a definite number of integral curves and is orthogonal to them. Moving along the flow lines, this area may isotropsically changes its size or being sheared or twisted, however it still holds the same number of flow lines. There are some analogies with elastic deformations. Here we should note that the evolution equations may be essentially regarded as identities, which become equations when they are for example used in space-time defined by Einstein field equations. Moreover, thee equations are of first order and non-linear. Also the expansion equation is the same as Riccati equation in mathematical regards[19]. The expansion is indeed the change of the cross-sectional area which is orthogonal to the geodesic (or non-geodesic) bundle.

Now for a detector which is falling on an integral curve in a weak gravitational system, the above formulations, do hold also when the waves impose small perturbations on the system. Regarding this, one can deal with the energy of the system, which the detector would feel. By using the advantage of the Hamilton-Jacobi equations, we have

$$g_{\mu\nu}p^\mu p^\nu + (mc)^2 = 0, \tag{8}$$

in which according to a parameterized trajectory bundle and in terms of the coordinates, p^μ is usually defined as[19]

$$p^\mu = \frac{dx^\mu}{d\tau} = \dot{x}^\mu \equiv u^\mu. \tag{9}$$

For a typical spherical metric

$$ds^2 = g_{00}(dx^0)^2 + g_{rr}dr^2 + r^2 d\Omega^2, \tag{10}$$

where $x^0 = ct$. For a conformal spherically symmetric metric, with $g_{00} = -B(r)$ and $g_{rr} = B(r)^{-1}$ where $B(r)$ is definitely dimensionless. One can write

$$\dot{x}^0 = \frac{a}{B(r)}. \tag{11}$$

For pure radial geodesics curves, this gives

$$-B(r)\left(\dot{x}^0\right)^2 + B(r)^{-1}\left(\dot{r}\right)^2 + mc^2 = 0, \tag{12}$$

Substitution of (11) and rearrangements result in

$$-\frac{1}{B(r)}\frac{a^2}{mc^2} + \frac{1}{B(r)}\frac{\dot{r}^2}{mc^2} + 1 = 0. \tag{13}$$

Since each part of (15) has to be dimensionless, therefore we require that

$$\mathrm{Dim}[a^2] = mc^2. \tag{14}$$

Equation (13), hinging on the energy definition $E = -g_{00}p^0$, could be also written in the form

$$-\frac{1}{B(r)}\frac{E^2}{mc^2} + \frac{1}{B(r)}\frac{(p^r)^2}{mc^2} + 1 = 0. \tag{15}$$

This shows an explicit dependence on energy of the curves for any kind of objects which move on such curves which also holds for a detector. In the next section, we will use these mathematical descriptions to describe a polarized gravitational wave equation and the consequent adjustments needed for the detectors to function appropriately.

3. The Polarization Limit and the Adjustments

One can derive all the results for vibrating, resonant detectors. To pattern the derivation after the treatment of the idealized detector we should let it be wave-dominated

($E_{\text{vibration}} \gg KT$). We can show that the displacements $\delta \mathrm{x} = \xi(\mathrm{x},t)$ of its mass elements are described by

$$\xi = \sum_n B_n(t)\mathbf{u}_n(x), \tag{16}$$

where the time-dependent amplitude for the nth mode satisfies the driven-oscillator equation

$$\ddot{B}_n + \frac{\dot{B}_n}{\tau_n} + \omega_n^2 B_n = R_n(t), \tag{17}$$

and where the curvature-induced driving term is

$$R_n(t) = -\int (\frac{\rho}{M}) u_n^j x^k d^3x = \frac{1}{4}\frac{\ddot{A}(I\!\!\!-_{(n)jk} e_{jk})}{M}. \tag{18}$$

To Fourier-analyze the amplitudes of the detector and waves, we have

$$B_n(t) = (2\pi)^{-\frac{1}{2}} \int_{-\infty}^{+\infty} \tilde{B}_n(\omega) e^{-i\omega t} d\omega, \tag{19}$$

$$A(t) = (2\pi)^{-\frac{1}{2}} \int_{-\infty}^{+\infty} \tilde{A}_n(\omega) e^{-i\omega t} d\omega,$$

and solve the equation of motion (18) and (19), to obtain, in the neighborhood of resonance,

$$\tilde{B}_n = \frac{\frac{1}{8}\frac{\omega_n \tilde{A}(I\!\!\!-_{(n)jk} e_{jk})}{M}}{|\omega| - \omega_n + \frac{1}{2}\frac{i}{\tau_n}} \qquad \text{for } \ |\omega \pm \omega_n| \ll \omega_n. \tag{20}$$

Also to calculate the total energy deposited in the detector by integrating

$$\begin{pmatrix}\text{energy}\\ \text{deposited}\end{pmatrix} = \int (\textbf{Force} \text{ per unit volume}) \cdot (\textbf{Velocity})\, d^3x dt. \tag{21}$$

Thereby we obtain

$$\begin{pmatrix}\text{energy deposited in}\\ n\text{th normal mode}\end{pmatrix} = \frac{1}{4}(I_{(n)jk} e_{jk}) \int \ddot{A}\dot{B}_n\, dt. \tag{22}$$

We apply Parseval's theorem and combine with expression (19) to obtain[20-23]

$$\begin{pmatrix}\text{energy deposited in}\\ n\text{th normal mode}\end{pmatrix} = \int \sigma_n(\nu) \mathcal{F}_\nu(\nu) d\nu. \tag{23}$$

where σ_n is given in[23], and (for $-\infty < \omega < +\infty$)

$$\mathcal{F}_\nu(\nu) = \mathcal{F}_\nu(\frac{\omega}{2\pi}) = \frac{1}{8}\omega^2 |\tilde{A}|^2. \tag{24}$$

It is shown that $\mathcal{F}_\nu(\nu)$ is the total energy per unit area per unit frequency carried by the waves past the detector[24,25]. One can obtain all the remaining cross sections by appropriate manipulations of this cross section[25]. In the next section, we use the mathematical tools for projecting out and integrating the transverse-traceless parts, which were developed the above discussions.

4. Solving the Wave Equations

The observed period of quadrupole vibration of the earth is 54 minutes[26,27]. To analyze that mode of vibration, with all due allowance for elasticity and the variation of density in the earth, is a major enterprise. Therefore, for a first estimate of the cross section of the earth for the absorption of quadrupole radiation, one can treat it as a globe of fluid of uniform density held in the shape of a sphere by gravitational forces alone (zero rigidity). Let the surface be displaced from $r = a$ to

$$r = a + a\alpha P_2(\cos\theta) \tag{25}$$

where θ is polar angle measured from the North Pole and α is the fractional elongation of the principal axis. The motion of lowest energy compatible with this change of shape is described by the velocity field

$$\xi^x = -\frac{1}{2}\alpha x, \qquad \xi^y = -\frac{1}{2}\alpha y, \qquad \xi^x = \alpha z, \tag{26}$$

which implies zero divergence and zero curl. The sum of the kinetic energy and the gravitational potential energy is derived as

$$E = -\left(\frac{3}{5}\right)\left(\frac{M^2}{a}\right)\left(1 - \frac{\alpha^2}{5}\right) + \left(\frac{3}{20}\right) Ma^2 \ddot{\alpha}^2. \tag{27}$$

This shows that the angular frequency of the free quadrupole vibration is

$$\omega = \left(\frac{16\pi}{15}\right)^{\frac{1}{2}} \rho^{\frac{1}{2}}. \tag{28}$$

The reduced quadrupole moments are

$$I\!\!\!-_{xx} = I\!\!\!-_{yy} = \frac{Ma^2\alpha}{5}, \qquad I\!\!\!-_{zz} = \frac{2Ma^2\alpha}{5}. \tag{29}$$

Therefore the rate of emission of vibrational energy, averaged over a period, is

$$-\left\langle \frac{dE}{dt} \right\rangle = \left(\frac{3}{125}\right) M^2 a^4 \omega^6 \alpha_{\text{peak}}^2. \tag{30}$$

In this regard, the exponential rate of decay of energy by reason of gravitational wave damping, or gravitational radiation line broadening, will be

$$A_{\mathrm{GW}} = \left(\frac{4}{25}\right) M a^2 \omega^4. \tag{31}$$

Finally, the resonance integral of the absorption cross section for radiation incident from random directions with random polarization is

$$\int \langle \sigma(\nu) \rangle d\nu = \left(\frac{\pi}{2}\right) \lambda\!\!\!^{-2} A_{\mathrm{GW}} = \left(\frac{2\pi}{25}\right) \frac{Ma^2}{\lambda\!\!\!^{-2}}. \tag{32}$$

By evaluating this resonance integral, this model of a globe of fluid of uniform density would imply for the earth, with average density 5.517 $\frac{\mathrm{gr}}{\mathrm{cm}^3}$, a quadrupole vibration period of 94 min, as compared to the observed 54 min; and a moment of inertia $(2/5)Ma^2$ as compared to the observed $0.33Ma^2$. These can be estimated as the correction factors for both effects and give for the final resonance integral $\sim 5\ \mathrm{cm}^2\mathrm{Hz}$.

5. Conclusion

We are considering a transverse-traceless configuration for a gravitational wave form, we calculated the perturbations for small displacements. This configuration was used in order to find applicable constructions for a gravitational wave detector, which is aimed to be installed in the solar system. The dynamic analysis of the idealized masses-on-spring detector, as developed in our investigations, is readily extended to a vibrating detector of arbitrary shape. The extension was carried out in Section 3 and its main results are summarized in Section 4. Part of the energy that goes into a detector is reradiated as scattered gravitational radiation. For any detector of laboratory dimensions with laboratory damping coefficients, this fraction is fantastically small. However, in principle one can envisage a larger system and conditions where the re-radiation is not at all negligible. In such an instance one is dealing with scattering. The attempt here, was made to analyze such scattering processes. For a simple order-of-magnitude treatment, one can use the same type of scattering formula that one employs to calculate the scattering of neutrons at a nuclear resonance or photons at an optical resonance. In conclusion, the detectors are heavily based on the stress-energy tensors of the system, which are imposed on the space-time geometry and consequently, on the geometric congruence.

6. Acknowledgements

This work has been supported by Payame Noor University.

7. References

1. Greene J, Bailyn CD, Orosz JA. Optical and Infrared Photometry of the Micro quasar GRO J1655-40 in Quiescence. The Astrophysical Journal. 2001; 551(2):1290-97. Crossref
2. Fabian AC, Pringle JE, Rees MJ. Tidal capture formation of binary systems and X-ray sources in globular clusters. Monthly Notices of the Royal Astronomical Society. 1975; 172:15-8. Crossref
3. Fabian AC, Ree MJ, Stella L, White NE. X-ray fluorescence from the inner disc in Cygnus X-1. Monthly Notices of the Royal Astronomical Society. 1989; 729:729-36. Crossref
4. Fabian AC. Broad line emission from iron K- and L-shell transitions in the active galaxy 1H 0707-495. Nature. 2009; 459:540-2. Crossref PMid:19478778.
5. Jiang J, Bambi C, Steiner JF. Using iron line reverberation and spectroscopy to distinguish Kerr and non-Kerr black holes. Journal of Cosmology and Astroparticle Physics. 2015; 5:25. Crossref
6. Jin C, Ward M, Done C, Gelbord J. A combined optical and X-ray study of unobscured type 1 active galactic nuclei - I. Optical spectra and spectral energy distribution modelling. Monthly Notices of the Royal Astronomical Society. 2012; 420(3):1825-47. Crossref
7. Esin AA, McClintock JE, Narayan R. Advection-Dominated Accretion and the Spectral States of Black Hole X-Ray Binaries. Application to Nova Muscae 1991. The Astrophysical Journal. 1997; 489(2):865-89. Crossref
8. Houck JC, Denicola LA. ISIS. An Interactive Spectral Interpretation System for High Resolution X-Ray Spectroscopy. Astronomical Data Analysis Software and Systems IX, ASP Conference Proceedings. 2000; 216:591.
9. Jin C, Done C, Middleton M, Ward M. A long XMM-Newton observation of an extreme narrow-line Seyfert 1. PG 1244+026. Monthly Notices of the Royal Astronomical Society. 2013; 436(4):3173-85. Crossref
10. Brenneman LW, Reynolds CS. Constraining Black Hole Spin via X-Ray Spectroscopy. The Astrophysical Journal. 2006; 652(2):1028-43. Crossref
11. Abbott PB. Observation of Gravitational Waves from a Binary Black Hole Merger. Physical Review Letters. 2016; 116:061102. Crossref1 Crossref2 Crossref3 PMid:26918975.
12. Fabian AC. Observational Evidence of Active Galactic Nuclei Feedback. Annual Review of Astronomy and Astrophysics. 2012 Jun; 50:455-89. Crossref
13. Greene JE, Ho LC. Active Galactic Nuclei with Candidate Intermediate-Mass Black Holes. The Astrophysical Journal. 2004; 61(2):722-36. Crossref
14. Hubeny I, Agol E, Blaes O, Krolik JH. Non-LTE Models and Theoretical Spectra of Accretion Disks in Active Galactic

Nuclei. III. Integrated Spectra for Hydrogen-Helium Disks. The Astrophysical Journal. 2000; 533(2):710-28. Crossref
15. Jin C, Ward M, Done C. A combined optical and X-ray study of unobscured type 1 active galactic nuclei - III. Broad-band SED properties. Monthly Notices of the Royal Astronomical Society. 2012; 425(2):907-29. Crossref
16. Brenneman LW. The Spin of the Supermassive Black Hole in NGC 3783. The Astrophysical Journal. 2011; 736(2):10. Crossref
17. Hubeny I, Blaes O, Krolik JH, Agol E. Non-LTE Models and Theoretical Spectra of Accretion Disks in Active Galactic Nuclei. IV. Effects of Compton Scattering and Metal Opacities. The Astrophysical Journal. 2001; 559(2):680-702. Crossref
18. Emmanoulopoulos D, McHardy IM, Papadakis IE. Negative X-ray reverberation time delays from MCG-6-30-15 and Mrk 766. Monthly Notices of the Royal Astronomical Society. Letters. 2011; 416(1):L94-8. Crossref
19. Emmanoulopoulos D, Papadakis IE, Dovciak M, McHardy IM. General relativistic modelling of the negative reverberation X-ray time delays in AGN. Monthly Notices of the Royal Astronomical Society. 2014; 439(4):3931-50. Crossref
20. Jamil O, Fender RP, Kaiser CR. iShocks. X-ray binary jets with an internal shocks model. Monthly Notices of the Royal Astronomical Society. 2010; 401(1):394-404. Crossref
21. Hubeny I, Lanz T. Non-LTE line-blanketed model atmospheres of hot stars. 1: Hybrid complete linearization/accelerated lambda iteration method. The Astrophysical Journal, Part I. 1995; 439(2):875-904. Crossref
22. Brenneman LW, Elvis M, Krongold Y, Liu Y, Mathur S. NGC 5548. Lack of a Broad Fe Kα Line and Constraints on the Location of the Hard X-Ray Source. The Astrophysical Journal. 2012; 744(1)(13):15.
23. Nayakshin S, Power C, King AR. The Observed M-σ Relations Imply That Super-massive Black Holes Grow by Cold Chaotic Accretion. The Astrophysical Journal. 2012; 753(1):7. Crossref
24. Narayan R, Yi I. Advection-dominated accretion. A self-similar solution. The Astrophysical Journal. 1994; 428(1): L13-6. Crossref
25. Narayan R, Yi I. Advection-dominated accretion: Self-similarity and bipolar outflows. The Astrophysical Journal, Part I. 1995; 444(1):231-43. Crossref
26. Nayakshin S, Kazanas D, Kallman TR. Thermal Instability and Photoionized X-Ray Reflection in Accretion Disks. The Astrophysical Journal. 2000; 537(2):833-52. Crossref
27. Brito R, Cardoso V, Pani P. Springer: Berlin: Lecture Notes in Physics. 3rd edn. 2015.